Low Temperature Sensitization of Type 304 Stainless Steel Pipe Weld Heat Affected Zone

CHARLES G. SCHMIDT, ROBERT D. CALIGIURI,
LAWRENCE E. EISELSTEIN, SHARON S. WING, and DANIEL CUBICCIOTTI

Large-diameter Type 304 stainless steel pipe weld heat-affected zone (HAZ) was investigated to determine the rate at which low temperature sensitization (LTS) can occur in weld HAZ at nuclear reactor operating temperatures and to determine the effects of LTS on the initiation and propagation of intergranular stress corrosion cracks (IGSCC). The level of sensitization was determined with the electrochemical potentiokinetic reactivation (EPR) test, and IGSCC susceptibility was determined with constant extension rate tests (CERT) and actively loaded compact tension (CT) tests. Substructural changes and carbide compositions were analyzed by electron microscopy. Weld HAZ was found to be susceptible to IGSCC in the as-welded condition for tests conducted in 8-ppm-oxygen, high-purity water at 288 °C. For low oxygen environments (*i.e.*, 288 °C/0.2 ppm O_2 or 180 °C/1.0 ppm O_2), IGSCC susceptibility was detected only in weld HAZ that had been sensitized at temperatures from 385 °C to 500 °C. Lower temperature heat treatments did not produce IGSCC. The microscopy studies indicate that the lack of IGSCC susceptibility from LTS heat treatments below 385 °C is a result of the low chromium-to-iron ratio in the carbide particles formed at grain boundaries. Without chromium enrichment of carbides, no chromium depleted zone is produced to enhance IGSCC susceptibility.

I. INTRODUCTION

A major corrosion problem in boiling water reactors (BWR's) is intergranular stress corrosion cracking (IGSCC) in the weld heat affected zone (HAZ) of Type 304 stainless steel pipes in recirculation systems and, to a lesser extent, in core spray systems. IGSCC first occurred in the weld HAZ of 10- and 25-cm-diameter piping, and, eventually, in large-diameter (*e.g.*, 61-cm) primary coolant lines. The slower development of IGSCC in the weld HAZ of large diameter pipe is attributed to the lower level of residual stresses that result from welding.[1]

For BWR pipe cracking, as for stress corrosion cracking in general, three conditions are necessary: a sensitized microstructure, a critical level of stress (or stress intensity), and an aggressive environment.[2] Combating stress corrosion invariably depends on alleviating one or more of these conditions. Approaches that have been investigated for reducing the cracking of BWR piping include improved weld design to reduce residual stresses from welding, improved water chemistry control to reduce the impurity content to acceptably low levels, and use of alternative alloys that are inherently immune to stress corrosion in BWR service environments.[3]

A sensitized microstructure is obtained when a stainless steel is held in a critical temperature range (usually 550 °C to 800 °C) long enough to allow the grain boundary chemistry to change. In stainless steels containing relatively high levels of carbon (0.04 to 0.07 pct), this change can be the precipitation of chromium-rich carbides at the grain boundaries.[4,5,6] Chromium carbide precipitation is accompanied by chromium depletion adjacent to the grain boundaries; this, in turn, can inhibit passivation which accelerates attack from aggressive environments near the grain boundaries. Concurrent with chromium carbide precipitation, grain boundary segregation of impurities such as sulfur and phosphorus can occur which might also enhance the susceptibility of grain boundaries to chemical attack.[7,8,9]

It has been suggested[10,11] that Type 304 stainless steel may be sensitized at relatively low temperatures (350° to 500 °C) if carbide nuclei are first formed in the normal sensitization temperature range (typically 550° to 800 °C, but dependent on alloy composition and cold work). The chromium depletion accompanying the formation of the nuclei is not sufficient to cause severe sensitization; however, once the nuclei are formed, they are able to grow at temperatures below the normal sensitization range and thus increase the degree of sensitization. The combination of the nucleating heat treatment and the subsequent prolonged low temperature heat treatment has been termed low temperature sensitization (LTS). Reversing the order of the heat treatments does not produce sensitization because carbides are not nucleated in the lower temperature range.

The objective of this study was to determine the kinetics of LTS and the effect of LTS on IGSCC susceptibility under conditions that approach those found in BWR piping.

II. EXPERIMENTAL PROCEDURE

Experiments were conducted on specimens machined from the weld HAZ of a 60-cm-diameter Type 304 stainless steel solution annealed pipe with a 3.08-cm-wall thickness. The chemical composition of the pipe in weight percent was 0.068C, 1.52Mn, 0.013P, 0.027S, 0.92Si, 18.62Cr, 8.43Ni, 0.20Mo, 0.31Cu, 0.17Co, with the balance Fe. The pipe was cut into 61-cm-long pipe lengths and welded back together by automatic gas tungsten arc welding using a total of 22 passes with ER 308 weld filler metal. Temperatures during welding were measured with thermocouples spot welded on the inner and outer surfaces of the pipe near the

CHARLES G. SCHMIDT, Materials Scientist, ROBERT D. CALIGIURI, Program Manager, LAWRENCE E. EISELSTEIN, Metallurgist, and SHARON S. WING, Chemist, are with SRI International, Menlo Park, CA 94025. DANIEL CUBICCIOTTI, Project Manager, is with Electric Power Research Institute, Palo Alto, CA 94304.

Manuscript submitted August 4, 1986

weld joint. At a distance of 0.3 cm from the weld fusion line, the inner surface of the pipe spent 180 to 220 seconds within the critical range for sensitization (above 550 °C). Temperature profiles during welding at the outer surface of the pipe 0.3 cm from the weld fusion line indicate that less than 30 seconds was spent 550 °C. The thermal exposure at the inner surface of the pipe was more severe because of the limited volume of base metal that was available to dissipate the heat of welding from the first few weld passes.

After welding, the pipe was sectioned so that LTS heat treatments could be performed on specimens from the welded pipe. The specimens were vacuum encapsulated in quartz and were heat treated at temperatures ranging from 280° to 500 °C for times of 1 to 9500 hours.

Electrochemical potentiokinetic reactivation (EPR) test specimens in the shape of parallelopipeds 1 × 1 × 6.5 cm were cut from the inside and outside surfaces of the pipe wall. The long dimension of these specimens traversed the weld metal and the HAZ on both sides of the weld. A suitable surface for EPR testing was obtained by milling the specimens just enough to flatten the original inside or outside pipe wall. This ensured that sensitized conditions very near the inner and outer surfaces of the pipe were measured. These flat surfaces were then wet ground to a 600-grit finish and polished with 6- and 1-μm diamond paste. The polished surface was masked with electroplater's tape to cover all areas except a small window either 10 × 4 mm or 10 × 2 mm.

Figure 1 shows the specimen dimensions and window locations used for the EPR tests. The EPR test procedure conformed to the specifications given by Clarke, Cowan, and Walker.[12] Duplicate tests were conducted for each heat treatment condition and pipe location.

With the EPR method, a specimen is subjected to a potentiokinetic potential sweep from a noble to an active potential in a deaerated solution of 0.5 M H_2SO_4 + 0.01 M KCNS. At the initial noble potential, the currents are low, consistent with the presence of a passive surface film. The area under the reactivation peak on the current-potential curve (*i.e.*, the number of coulombs passed per cm^2) is proportional to the degree of sensitization and is referred to as P_a. If sensitization is low, the reactivation peak will be small and currents will remain low and typical of passive metals. If sensitization is extensive, the reactivation peak will be large and currents will be high and typical of active metals.

For the transmission electron microscopy (TEM) and scanning transmission electron microscopy (STEM) studies, specimens were taken 2 to 10 mm from the weld fusion line near the inner diameter of the pipe. Twin jet polishers were used with 10 pct perchloric acid/90 pct 2-butoxyethanol to obtain thin foils. Microscopy was performed at Stanford University using a Phillips EM 400 STEM instrument and at the University of Cincinnati using a JEOL 200A TEM and a JEOL 100 CX STEM instrument. Microanalysis by STEM was conducted on material in the as-welded condition in the vicinity of carbides near the plane of maximum sensitization in the HAZ to determine the degree of chromium depletion adjacent to these carbide particles. In all of the STEM analyses, the spatial resolution was estimated to be ±25 nm and the compositional resolution was about 0.25 wt pct.

Constant extension rate tests (CERT) and compact tension (CT) crack growth rate tests were performed in simulated BWR water with controlled amounts of dissolved oxygen. A recirculating water loop was constructed to control and verify water conductivity, dissolved oxygen content, pressure, temperature, and flow rate. Water flow-

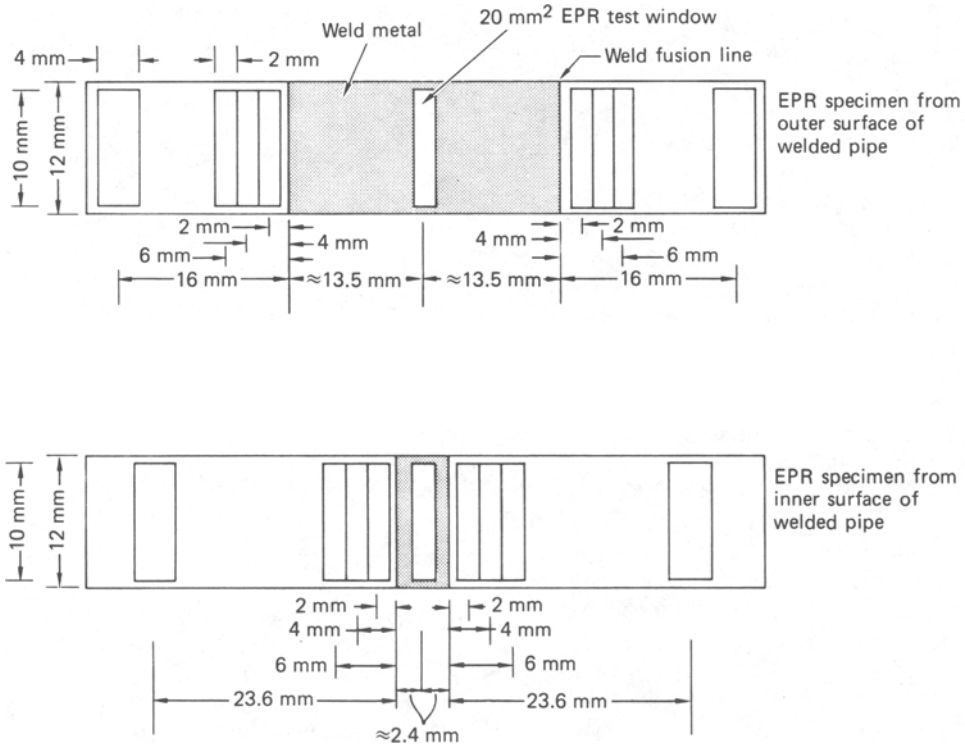

Fig. 1—Dimensions of electrochemical potentiokinetic reactivation (EPR) test specimens taken from near the inner and outer surface of 61-cm-diam (24-in.), Schedule 80, Type 304 stainless steel welded pipe

ing into the 2-liter, HASTELLOY* C test autoclave had a conductivity of 0.06 μS/cm; the autoclave effluent conductivity was typically 0.5 to 1.0 μS/cm. After passing through a pressure reduction valve, the water flowed into a holding tank where an oxygen/nitrogen gas mixture was used to maintain the required dissolved oxygen content. Oxygen content was monitored by in-line oxygen analyzers or by colorimetry on water samples. Water conductivity was maintained with mixed bed filters. A water flow rate of four liters per hour and a pressure of 8 MPa (1400 psi) was maintained in the test autoclave.

*HASTELLOY is a trademark of Cabot Corporation.

CERT specimens were machined from blanks cut from the welded pipe described above. The gage length of each CERT specimen traversed the weld and the weld HAZ near the inner diameter of the pipe. Round bar specimens were used with 50.8 mm gage lengths and 6.35 mm gage diameters. CERT's were conducted at initial strain rates of 1×10^{-6} to 1.3×10^{-6} s^{-1} and temperatures of 180 °C or 288 °C in high purity water containing 0.2, 1, or 8 ppm dissolved oxygen.

CT specimens were specially designed to permit the measurement of the crack growth rate in the weld HAZ near the inner diameter of the pipe. By electron beam welding additional pipe base metal to the inside pipe wall, blocks of material of sufficient size to produce ¾T-compact tension specimens (see Figure 2) were obtained with proportions that conform to ASTM E-399.[13] The depth of the notch plus the fatigue precrack was chosen so that the electron-beam weld joint and HAZ would not interfere with the determination of the crack growth rate of the pipe weld HAZ. A compliance calibration curve was generated to ensure that standard compliance relations[14] could be used to determine crack length. For the crack growth rate tests in simulated BWR water, a water immersible displacement gage was attached to the front face of the CT specimens. Crack length was measured by compliance measurements during partial unloading and reloading. These measurements were performed approximately five times per week. Crack growth rates were adjusted to conform to the initial and final crack length measurements determined from fractographic examination of the specimen.[13]

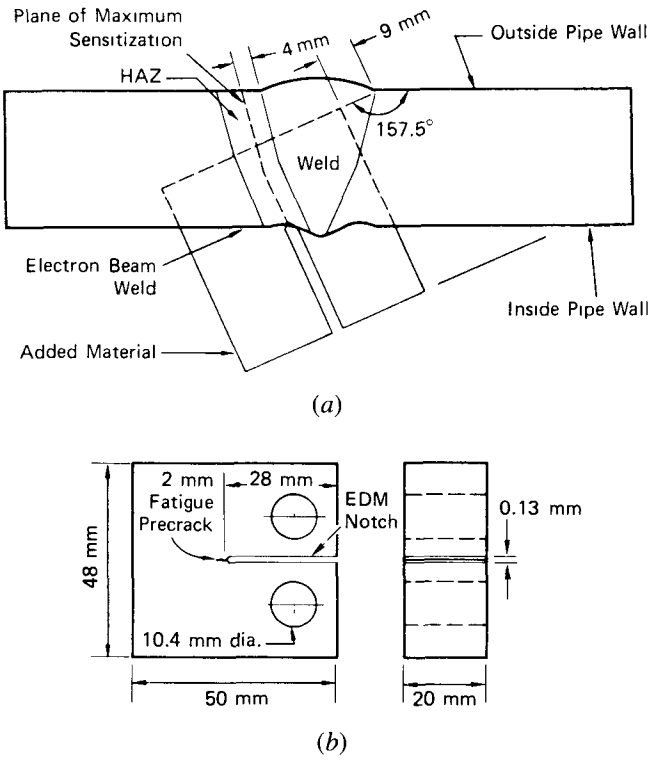

Fig. 2—CT specimen dimensions.

III. RESULTS

A. *Electrochemical Potentiokinetic Reactivation (EPR) Tests*

The dependence of the degree of sensitization, P_a, on the distance from the weld fusion line and time and temperature of LTS heat treatments is shown in Figures 3 and 4.

Figure 3 shows that LTS heat treatments at 500 °C caused larger increases in the degree of sensitization in the HAZ as the weld fusion line was approached. EPR data obtained from material farther away from the weld fusion line (16 to 23.6 mm) in the base metal show very low sensitization levels after welding that do not increase substantially with LTS heat treatment. The EPR data at different LTS heat-treatment temperatures are shown in Figure 4. The 500 °C LTS heat treatment produced substantially higher sensitization levels than the heat treatments at 400 °C and below. Figure 4 also shows that the degree of sensitization increased with increasing heat-treatment time. However, the increase is not a monotonic trend over time; rather, it is

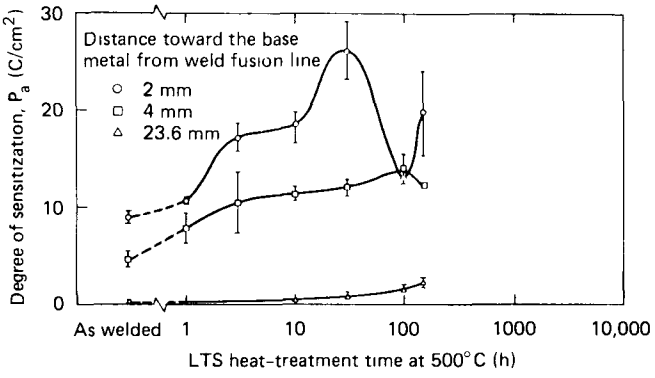

Fig. 3—EPR data from the inside surface of a Type 304 stainless steel weld HAZ after LTS at 500 °C.

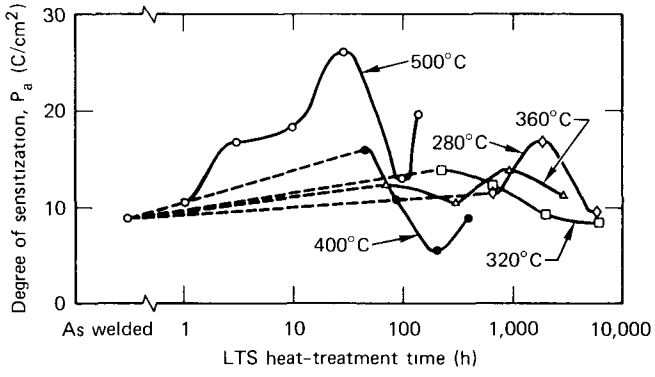

Fig. 4—EPR data from the inside surface of a Type 304 stainless steel pipe weld HAZ 2 mm from the weld fusion line after LTS.

punctuated by one or two maxima and minima. The most prominent maxima consistently occur at increasing LTS heat-treatment times as the LTS heat-treatment temperature is decreased.

The temperature dependence of the EPR data is displayed in Figure 5 in the form of an Arrhenius plot with the time to reach a reference level of sensitization (P_a = 15 °C/cm^2) as the independent variable. The reference sensitization level is an arbitrary value in the midst of the range of sensitization data that separates "high" and "low" sensitization levels. The critical time of sensitization was computed for each LTS heat-treatment temperature from an interpolation to the reference P_a value. An activation energy of 97 kJ/mole was obtained from the data in Figure 5.

B. *TEM Results*

Two examples of the appearance of grain boundary carbides in the weld HAZ are shown in Figure 6. A summary of the changes on carbide size with increasing LTS heat-treatment time and temperature is shown in Table I. In most cases, carbides were seen at high angle boundaries. No significant carbide growth from the as-welded condition was apparent after the LTS heat treatments at 280 °C or 320 °C. The 360 °C LTS heat treatments for 72 and 2592 hours increased carbide dimensions over the as-welded condition by factors of 2 and 4, respectively. The 400 °C LTS heat treatment for 48 hours produced less carbide growth than the long-term 360 °C heat treatment, and the 500 °C LTS heat treatments for 24 and 150 hours clearly resulted in the largest carbides.

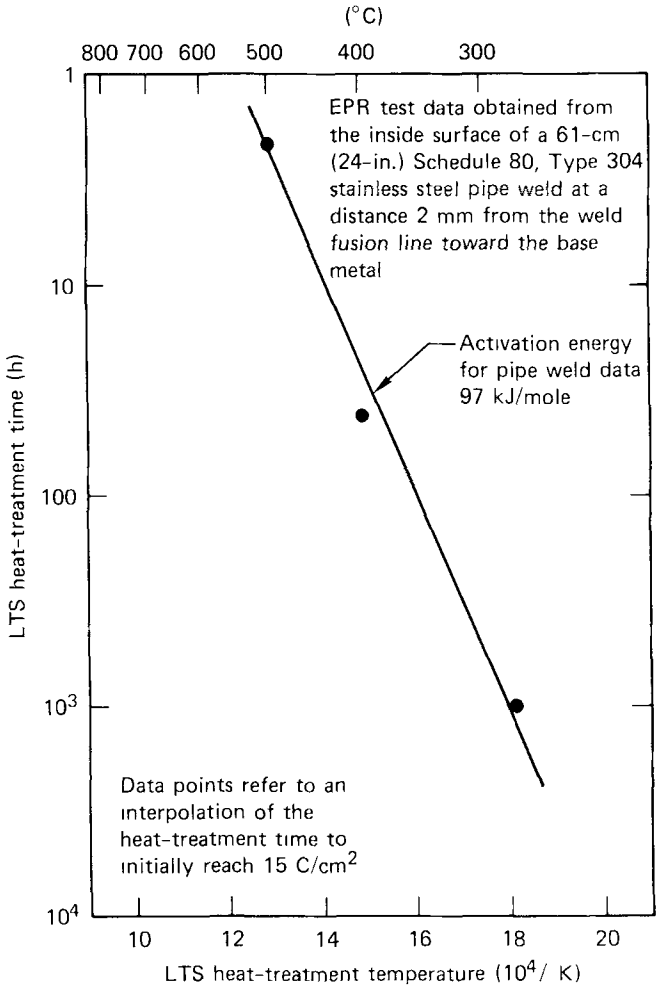

Fig. 5 — Arrhenius plot of the activation energy determined from EPR data at a critical P_a value of 15 °C/cm^2.

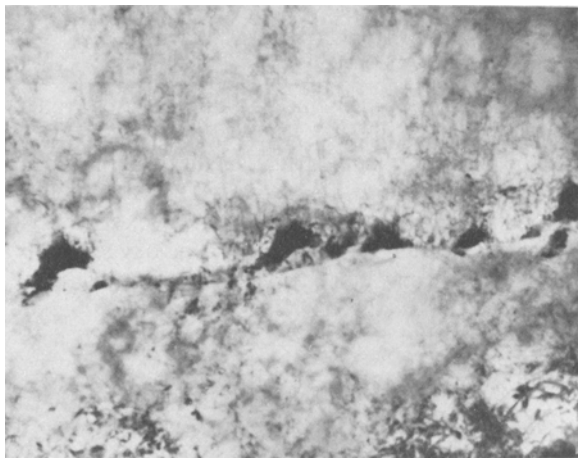

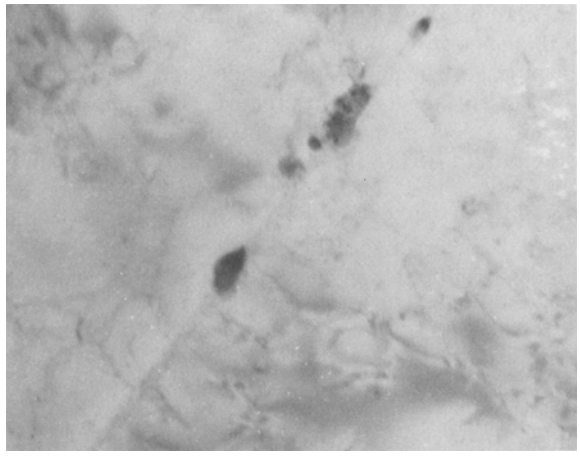

Fig. 6 — Typical TEM micrographs of grain boundary carbides after LTS heat treatment

Microanalysis by STEM of grain boundaries in weld HAZ in the as-welded condition revealed no significant gradient in chromium concentration although slightly depressed chromium content might exist for regions within 100 nm of the grain boundary (see Figure 7). Analysis of grain boundary carbide indicates a chromium concentration of 21 to 25 wt pct, although particle composition measurements might be influenced by both the carbide composition and the surrounding matrix composition.

The results of the STEM analyses across the grain boundaries in the samples with long-term low temperature heat

Table I. Representative Carbide Sizes for LTS Heat-Treated Weld HAZ

LTS Treatment	Distance from Weld Fusion Line*		
	2 mm	3 mm	4 mm
As-welded		50 nm by 20 nm	
280 °C/4968 h	30 to 40 nm in diameter		30 to 40 nm in diameter
320 °C/5832 h	30 to 40 nm by 100 nm		<5 nm in diameter
360 °C/72 h			70 to 90 nm by 100 nm
360 °C/2592 h	50 to 70 nm by 200 nm		40 to 60 nm by 200 nm
400 °C/48 h	120 to 150 nm by 40 nm		30 nm by 100 nm
500 °C/24 h		400-nm-wide continuous sheet	
500 °C/150 h			250 to 300 nm by 100 nm

*No carbides were observed 20 mm from the fusion boundary.

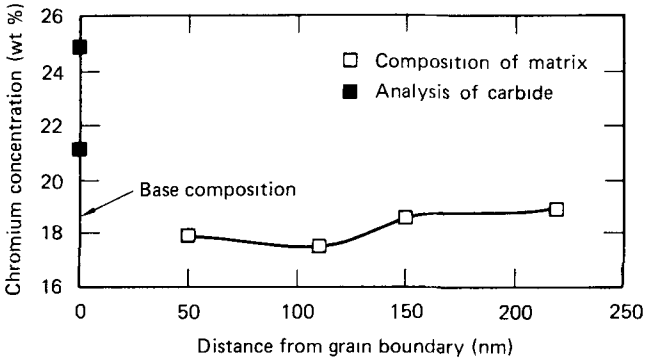

Fig. 7 — STEM analysis of the chromium concentration profile near a grain boundary 3 mm from the weld HAZ in as-welded condition.

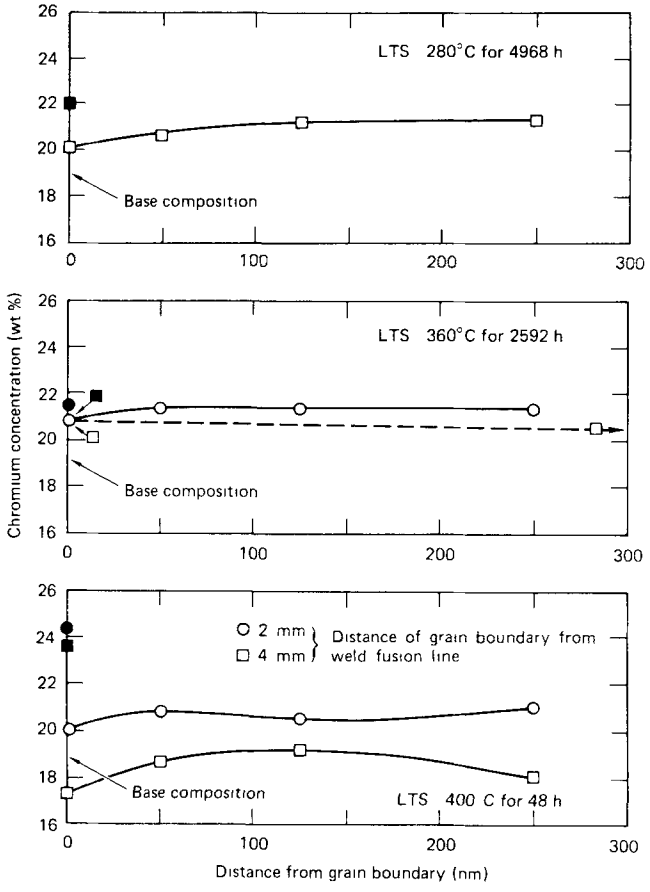

Open symbols – composition of matrix
Closed symbols – analysis of carbide

Fig. 8 — STEM analysis of chromium concentration profiles produced by LTS heat treatments

treatments are shown in Figure 8. Little or no chromium depletion was detected in the grain matrix adjacent to the grain boundaries. However, a variation in the chromium concentration of the carbides was detected that might be significant. The 400 °C LTS heat treatment for 24 hours produced carbides with chromium concentrations that were higher than the matrix chromium concentration, whereas the 360 °C/2592-h and 280 °C/4968-h LTS heat treatments produced carbides with chromium concentrations that were roughly equal to the matrix chromium concentration.

The results of the STEM analyses across grain boundaries in samples with LTS heat treatments at 500 °C for 24 hours are shown in Figure 9. These results indicate that the chromium concentration at grain boundaries generally increased with decreasing distance from the weld fusion line. This is particularly evident in the foil removed 2.8 mm from the weld fusion line in which the elevated chromium concentration in the grain boundary extends over about 400 nm.

The results also show that there is no substantial chromium depletion in the matrix adjacent to grain boundaries even for grain boundaries as close as 2.8 mm from the weld fusion line. Although the LTS treatment of 500 °C for 24 hours caused the grain boundary carbides to grow, it did not substantially modify the microchemistry of the matrix adjacent to the grain boundary carbides. It is possible, of course, that significant chromium depletion occurred adjacent to the carbide/matrix interface over distances below the spatial resolution of the STEM analyses (<25 nm).

C. *CERT Results*

The CERT results are summarized in Table II. The reason for conducting the CERT's was to identify the regions around the weld with high IGSCC susceptibility and to determine the LTS heat treatment conditions necessary to induce IGSCC.

1. *Determination and location of maximum IGSCC susceptibility*

Comparison of the inside pipe wall specimens shows that the 500 °C LTS treatment for 24 hours significantly reduced the elongation to failure, reduction in area, and the ultimate tensile strength of the material relative to the as-welded condition. Hence, the pipe weld examined in this investigation was susceptible to IGSCC after LTS at 500 °C for 24 hours but not in the as-welded condition. A similar but

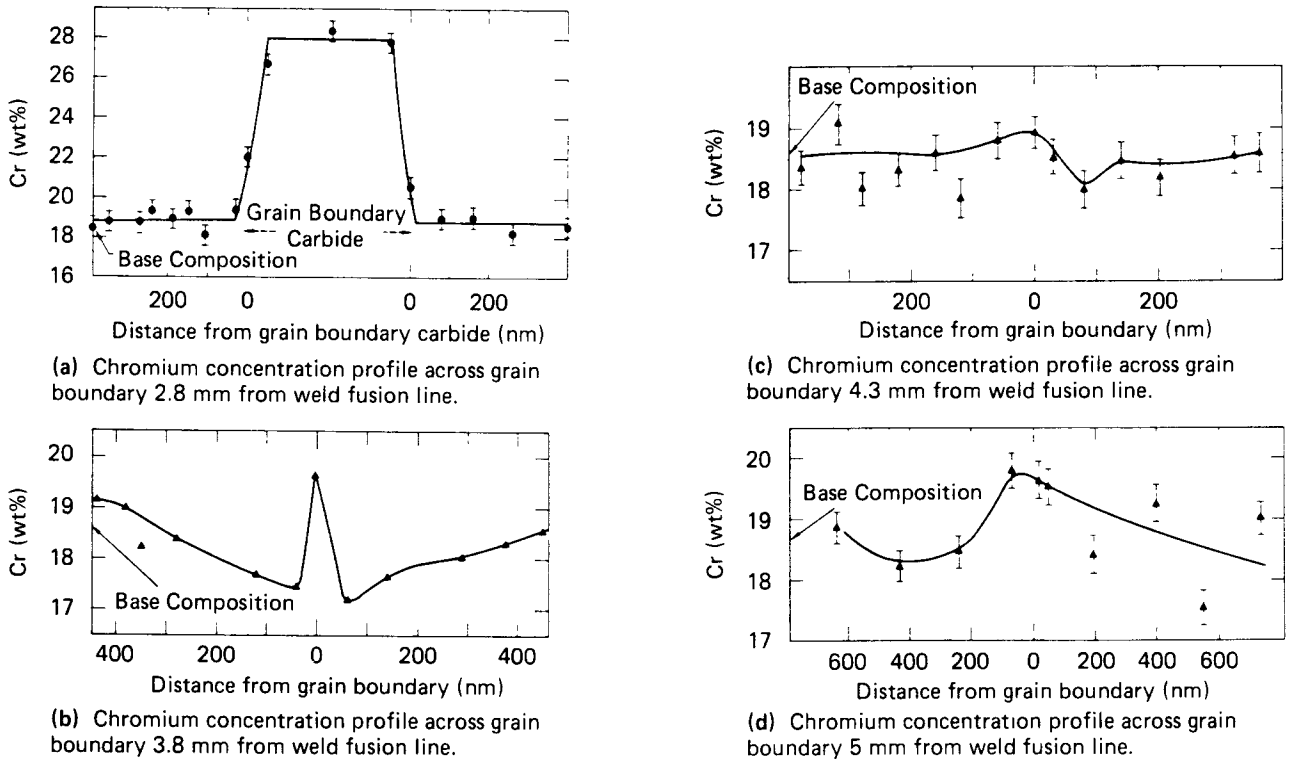

(a) Chromium concentration profile across grain boundary 2.8 mm from weld fusion line.

(c) Chromium concentration profile across grain boundary 4.3 mm from weld fusion line.

(b) Chromium concentration profile across grain boundary 3.8 mm from weld fusion line.

(d) Chromium concentration profile across grain boundary 5 mm from weld fusion line.

Fig. 9—STEM analysis of weld HAZ 4.3 to 5 mm from the weld fusion line with an LTS treatment of 500 °C for 24 h.

Table II. Summary of Constant Extension Rate Tests (CERTS) on Welded Type 304 Stainless Steel Pipe in Simulated BWR Water

Heat Treatment after Welding (°C/h)	Test Environment °C/ppm O_2	Failure Location	Elongation to Failure	Maximum Reduction in Area (Pct)	Maximum Stress MPa (Ksi)
As-welded	288/8	weld metal	0.25	76	524 (76)
As-welded[a]	288/8	weld metal	0.23	75	503 (73)
As-welded[b]	288/8	HAZ[c]	0.16	29	496 (72)
280/1656[b]	180/1	base metal	0.25	76	352 (51)
280/1656[b]	288/8	HAZ[c]	0.18	39	386 (56)
320/1944	288/0.2	weld metal	0.21	59	372 (54)
320/1944[b]	288/6	HAZ[c]	0.11	35	310 (45)
360/96	180/1	weld metal	0.33	56	402 (67)
360/96	288/0.2	base metal	0 36	59	490 (71)
360/288[b]	180/1	base metal	0.35	69	— (—)
360/288	288/0.2	weld metal	0.29	51	462 (67)
360/864[b]	180/1	base metal	0.35	64	455 (66)
360/864	288/0.2	weld metal	0.36	51	469 (68)
360/2592[b]	180/1	base metal	0.25	82	407 (59)
360/2592[b]	288/6	HAZ[c]	0.14	44	462 (67)
400/48	288/0.2	base metal	0.25	67	469 (68)
400/96	288/0.2	HAZ[c]	0.21	29	466 (67)
400/192	288/0.2	HAZ[c]	0.21	29	452 (66)
400/384	288/0.2	HAZ[c]	0.16	20	451 (65)
500/10	288/0.2	—	0.26	75	452 (65)
500/24	288/8	HAZ[c]	0.12	24	476 (69)
500/24[a]	288/8	HAZ[c]	0.20	22	490 (71)
500/30	288/0.2	HAZ[c]	0.20	23	308 (45)
500/100	288/0.2	HAZ[c]	0.10	—	186 (27)
500/150	288/0.2	HAZ[c]	0.05	—	162 (24)

[a]Specimen machined from material near outside wall of welded pipe All others from material near inside wall.
[b]Specimen was electropolished. All other specimens were mechanically polished to 600 grit
[c]Specimen fracture surface indicated presence of IGSCC All other specimens had completely ductile fracture surfaces

less pronounced effect of LTS was observed for specimens from the outer pipe wall.

The elongation to failure and maximum strength values are about the same for the as-welded and the 500 °C/24 h LTS-heated conditions, but the 500 °C LTS treatment significantly lowered the reduction in area.

Table III shows that specimens with fracture surfaces that did not exhibit IGSCC broke in the weld filler metal or the base metal. Those specimens with LTS heat treatments severe enough to cause IGSCC broke in the HAZ 2 to 4 mm from the weld fusion line. Secondary cracks initiated on the surface of both specimens in the HAZ, but these eventually stopped without penetrating very far. The region of high sensitization indicated by the CERT results is 2 to 4 mm from the weld fusion line in the weld HAZ. This region corresponds to the location of high temperatures (>500 °C) measured during temperature profiling and the location of high EPR readings.

2. *Critical LTS heat treatments for IGSCC*

For the specimens given LTS heat treatments at 500° and 400 °C for various times, it is evident from the ductility data in Table II that IGSCC susceptibility in the 288 °C/0.2-ppm-O_2 environment first occurs for LTS heat treatments between 48 and 96 hours at 400 °C and between 10 and 30 hours at 500 °C.

IGSCC was not observed in material with LTS treatments at 360 °C for the CERT's performed in the 288 °C/0.2 ppm O_2 environment. This indicates that more than the maximum heat treatment time investigated (864 hours) is required at 360 °C before IGSCC susceptibility is reached. However, it is reasonable to assume that IGSCC would not be observed for this environment even after 2592 hours of heat treatment at 360 °C in view of the ductile fracture that was obtained in the 180 °C/1.0-ppm-O_2 environment. Increasing the oxygen content at a fixed temperature increases the susceptibility to IGSCC, and decreasing the temperature to 180 °C at a fixed oxygen content also increases the susceptibility.[15] Therefore, the combination of 288 °C/0.2 ppm O_2 represents the least aggressive simulated BWR environment examined.

The CERT that was run in 288 °C water with 6.0 ppm O_2 exhibited IGSCC after 2592 hours of heat treatment at 360 °C; the occurrence of IGSCC in this case is undoubtedly a consequence of the high oxygen content in the environment. No IGSCC was observed on the fracture surfaces of the specimen with the same LTS heat treatment that was tested in 180 °C water with 1.0 ppm O_2.

The two CERT's on material with LTS heat treatments at 320 °C indicate that IGSCC susceptibility is reached after 1944 hours of heat treatment in 288 °C water with 0.2 ppm O_2. IGSCC was induced by increasing the oxygen content to 6.0 ppm; however, differences in specimen surface preparation may have also contributed to the increased susceptibility.

The two CERT's run on specimens with LTS heat treatments at 280 °C for 1656 hours were tested in the 1-ppm-O_2 and 8-ppm-O_2 environments because an LTS heat treatment at a higher temperature for a longer time did not exhibit IGSCC in the 0.2-ppm-O_2 environment. IGSCC was evident only in the test environment containing 8.0 ppm O_2; the fracture surface of the specimen tested in 180 °C water with 1.0 ppm O_2 was completely ductile. Nevertheless, SEM examination of the gage length near the fracture surface of the specimen tested in the 180 °C/1-ppm-O_2 environment did reveal the initiation of intergranular cracking as shown in Figure 10. Apparently, the combination of sensitization heat treatment and environment imposed on this specimen

Table III. Comparison of Three Methods of Determining IGSCC Susceptibility in Type 304 Stainless Steel Weld HAZ

Compact Tension Specimen Crack Growth Rate			Constant Extension Rate Test Results			EPR Degree of Sensitization Results		
							Distance from Weld Fusion Line	
LTS Condition (°C/h)	Environment (°C/ppm O_2)	Relative IGSCC Rate	LTS Condition (°C/h)	Environment (°C/ppm O_2)	Occurrence of IGSCC	LTS Condition (°C/h)	2 mm (C/cm^2)	4 mm (C/cm^2)
400/384[a]	180/1	high	400/384	288/0.2	yes	400/384	9.06 8.49	7.66 3.92
500/24[a]	180/1	high	500/30	288/0.2	yes	500/30	29.2 23.1	12.9 11.2
385/360 to 385/1440	180/1 and 288/0.2	intermediate	—	not available	—	—	not available	—
360/720 to 360/2880	180/1 and 288/0.2	very little	360/2592	180/1	no	360/2592	15.9 7.11	9.74 4.45
335/5040 to 335/9528	180/1 and 288/0.2	none	320/1944	288/0.2	no	320/1944	7.02 11.6	4.88 9.00
—	not available	—	280/1656	180/1	no	280/1656	18.4 13.9	11.9 9.8
As-welded	180/1 288/0.2	none	as-welded	288/1	no	as-welded	9.43 8.34	5.48 3.86

[a]The crack growth rate trends for the 500 °C and 400 °C LTS heat treatment condition cross The crack growth rate ranking shown above for these two conditions is appropriate at high and low stress intensities (but not intermediate levels).

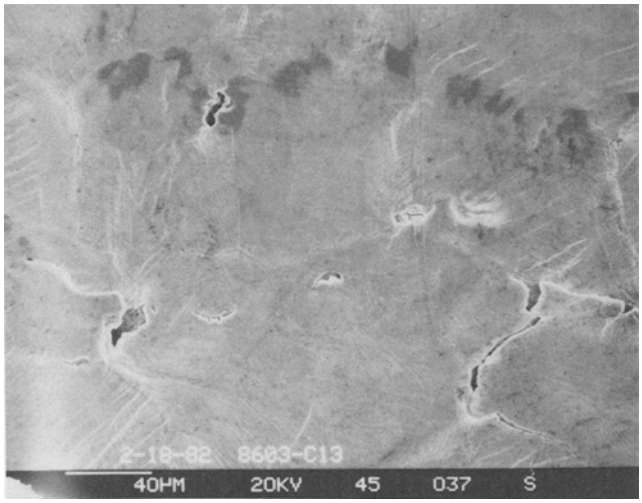

Fig. 10 — SEM of the gage length of CERT specimen heat treated at 280 °C for 1656 h and tested in 1 ppm oxygenated water at 180 °C.

was sufficient for initiation of IGSCC, but not propagation. A similar situation (*i.e.*, crack initiation but little propagation) was observed for the specimen heat treated at 360 °C for 2592 hours and tested in 180 °C water with 1.0 ppm O_2.

D. *Compact Tension Crack Growth Rate Tests*

The compact tension experimental results are summarized in Figure 11. The objective of the CT experiments was to assess the effect of LTS heat treatments and environment on IGSCC crack propagation rate.

1. *Effect of LTS heat treatment on IGSCC growth rate*

For 180 °C water with 1.0 ppm O_2, the highest IGSCC rates were produced by the 400 °C LTS heat treatment except at intermediate stress intensity levels where the 500 °C LTS heat-treated specimen cracked most rapidly (see Figure 11). The 385 °C LTS heat treatments produced significantly lower IGSCC growth rates than the 400° or 500 °C LTS heat treatments at high stress intensities ($K \gtrsim 40$ MPa$\sqrt{m}$); however, the difference at low stress intensities was small. The 385 °C LTS heat treatments showed a small increase in crack growth rate (factor of 6) as stress intensity was increased to 50 MPa$\sqrt{m}$. The 400° and 500 °C LTS heat treatments produced a substantial increase in crack growth rate (over a factor of 10) as stress intensity was increased from 30 to about 38 MPa$\sqrt{m}$. For LTS heat treatments at 335 °C, no IGSCC was observed in the 180 °C/1.0 ppm O_2 environment or the 288 °C/0.2 ppm O_2 environment. No consistent differences in IGSCC susceptibility or rate were observed as a function of heat treatment time for any of the heat treatment temperatures.

The results in Table III show the effect of LTS heat treatment on IGSCC susceptibility as determined from the crack growth rate tests and the CERT's. Table III also shows the degree of sensitization as measured in the EPR tests. The CERT results are consistent with the crack growth results insofar as both tests indicate substantial IGSCC after LTS heat treatments at 500° and 400 °C, but little or no IGSCC after LTS heat treatments at 360 °C or below. The trends displayed by the EPR results vary from the trends of the crack growth measurements. For the 400°, 360°, and 335 °C LTS heat-treated conditions and the as-welded condition, the EPR measurements are approximately equal, whereas the CT tests show intermediate crack growth rates for the 385 °C LTS conditions, and no crack growth in the 360° and 335 °C LTS conditions. Furthermore, the 500 °C LTS heat treatment produced EPR readings considerably higher than the 400 °C LTS heat treatment, even though the crack growth rates from 500 °C LTS heat-treated material were generally lower.

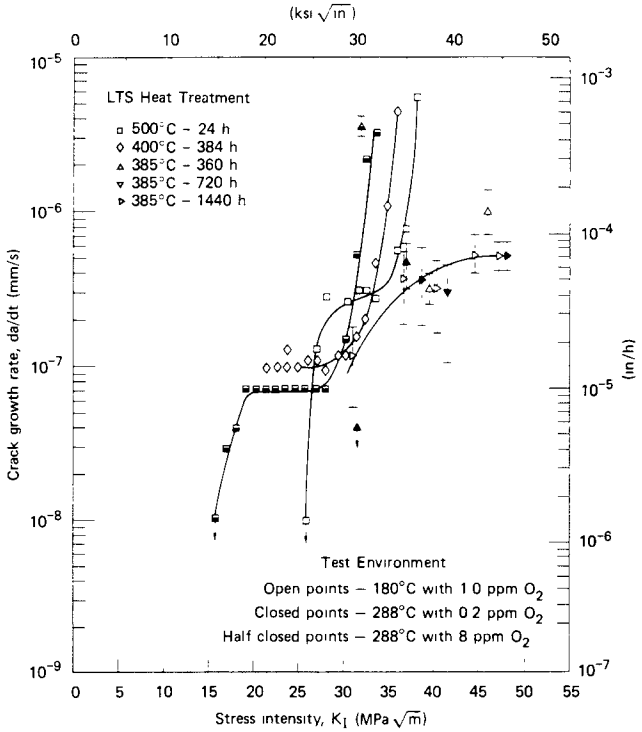

Fig. 11 — Crack growth rate of Type 304 stainless steel welded pipe HAZ in high purity water environments

2. *Effect of environment on IGSCC growth rate*

The highest crack growth rates for the high purity environments tested were from the 288 °C/8-ppm-O_2 environment. Crack growth was also observed for the as-welded condition in the high oxygen environment; however, the data are insufficient to estimate the rate of cracking. Confirmation of the IGSCC susceptibility of the as-welded material in the 8-ppm-O_2 environment is provided by the CERT data in which one failure by IGSCC occurred in an electropolished sample in the as-welded condition (see Table II). Materials subjected to either the 500 °C or the 385 °C/360-h LTS heat treatments cracked readily as a result of the high oxygen content. The effect of this environment is also reflected in the low plateau level and the crack growth at low stress intensities displayed by the 500 °C LTS condition.

Comparing the results of the 288 °C/0.2-ppm-O_2 environment with those from the 180 °C/1-ppm-O_2 environment does not indicate any remarkable differences. Tests performed on specimens in the as-welded condition revealed no crack growth in the 288 °C/0.2-ppm-O_2 environment or the 180 °C/1.0-ppm-O_2 environment. The 385 °C LTS heat-treated material appears to crack at a rate that is influenced only by stress intensity and not by the differences between the 288 °C/0.2-ppm-O_2 and 180 °C/1-ppm-O_2 environment.

IV. DISCUSSION

The effect of LTS heat treatment on sensitization is commonly attributed to grain boundary chromium depletion due to the growth of grain boundary carbides[4,5,6] or enhanced grain boundary attack due to impurities at grain boundaries.[7,8,9] The EPR, CERT, and CT results from the present experiments indicate that the occurrence of IGSCC from LTS heat treatment is not simply related to chromium diffusion kinetics. For example, in Figure 5, the activation energy that corresponds to the temperature dependence of the EPR data is 97 kJ/mole. This value does not agree with chromium activation energies commonly associated with sensitization processes (*i.e.*, 280 kJ/mole for lattice diffusion or 170 kJ/mole for grain boundary diffusion).[16]

From the CERT's and CT tests, the temperature dependence for the appearance of IGSCC is shown in Figure 12. The criterion for considering a specimen to be susceptible to IGSCC was the appearance of any intergranular cracking on the fracture surface after testing in a 228 °C/0.2-ppm-O_2 or 180 °C/1-ppm-O_2 water environment. Susceptibility indications from CT tests performed at General Electric Company[17] for sensitization treatments of weld HAZ at 621 °C are also shown in Figure 12. The CERT and CT results are highly compatible; both show no susceptibility for LTS heat treatments at 360 °C and below. LTS heat treatments at higher temperatures produced IGSCC in all cases with the exception of two CERT's that were exposed to very short-term heat treatments.

The bilinear correlation separating the IGSCC susceptible conditions from the nonsusceptible conditions indicates activation energies of 420 kJ/mole and 86 kJ/mole for the high and low temperature regimes, respectively. The latter activation energy is in fair agreement with that observed from the EPR data; however, neither value agrees with the activation energy for chromium matrix or grain boundary diffusion cited above.

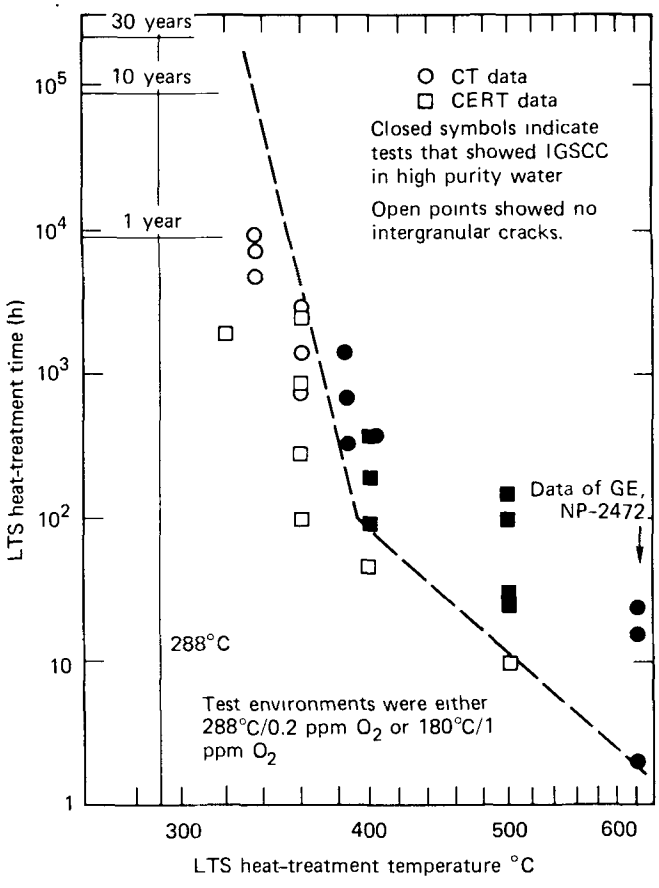

Fig. 12—LTS time-temperature dependence of IGSCC based on CT data.

The descriptions of carbide size and chemistry in the previous section appear to be consistent with the occurrence of IGSCC susceptibility indicated by the CERT and CT tests. Little or no carbide growth was detected for LTS heat treatments at or below 320 °C. Similarly, no IGSCC susceptibility in the CERT and CT tests occurred in this temperature range. The 360 °C LTS heat treatment produced carbide growth but no IGSCC susceptibility; however, the chromium content of these carbides was no higher than that of the matrix (see Figure 8). This suggests that chromium depletion of the matrix (and, therefore, IGSCC susceptibility) might not have increased after an LTS heat treatment at 360 °C even though carbide dimensions increased slightly.

A low chromium content of carbides will limit the size of the chromium depleted zone that surrounds the carbide. This, in turn, might reduce the degree of sensitization that results from carbide precipitation. Variations in the chromium content of grain boundary carbides as a function of sensitization temperature have not been considered in the models of sensitization; however, this might be an important factor that will explain some of the discrepancies between the models and EPR results.

Microprobe analyses of extraction replicas with $M_{23}C_6$ precipitates formed by aging austenitic stainless steel have been reported by Da Casa *et al.*[18] and by Philibert *et al.*[19] The "commercial" steel investigated by Da Casa *et al.* had a composition similar to the present material (0.07 pct C). They found that in the temperature range of 700° to 800 °C and for times of one to 500 hours, the Cr/Fe ratio increased with both aging temperature and time. The increase was rapid for short times, but slowed considerably. The results suggest that the Cr/Fe ratio would reach a temperature dependent saturation value.

From the data of Da Casa *et al.*, we show the atom fraction of Cr in $(Fe, Cr)_{23}C_6$ as a function of the reciprocal of the absolute temperature (see Figure 13). Their data for 500 hours of aging are represented by filled squares. (Their results for 24 hours' aging on the same scale are only slightly below the 500-hour points, indicating that aging time beyond 24 hours has little effect on the curve.) Also included in Figure 13 are the atom fractions of Cr in the carbide precipitates obtained in the aged pipe welds of the present work.

The two sets of data might be represented by the full line in Figure 13 (which consists of two intersecting straight lines). At the higher temperatures, the chromium fraction increases with temperature and reaches pure $Cr_{23}C_6$ at about 880 °C. As the temperature is decreased, the chromium fraction in the precipitates decreases until it reaches a value approximately equal to that in the base alloy. That temperature is about 450 °C. With further decrease in temperature, the atom fraction of Cr in the precipitate does not change and continues to be approximately equal to the atom fraction of Cr in the base metal.

Growth of $M_{23}C_6$ during thermal aging involves two parallel processes. In one, chromium enrichment of carbides

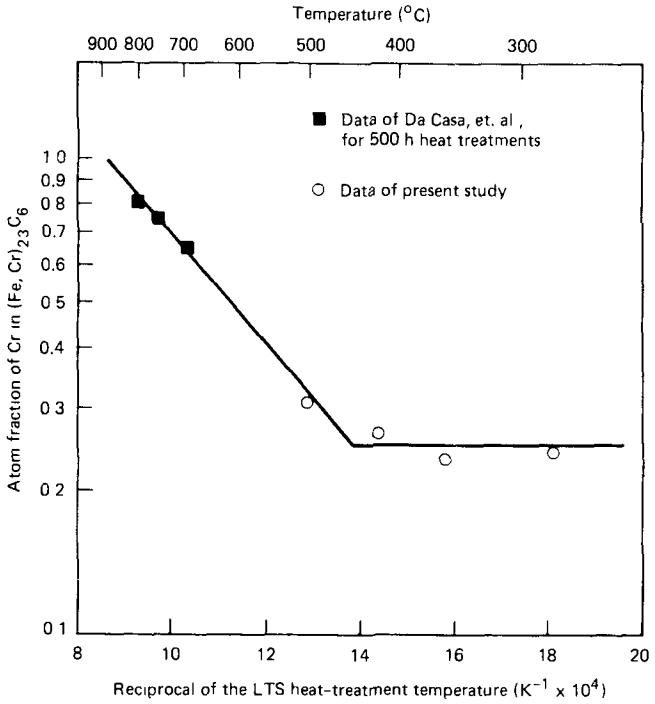

Fig. 13 — Effect of LTS heat treatment temperature on the atom fraction of chromium in $(Fe, Cr)_{23}C_6$.

(compared to the matrix) occurs at a rate that is controlled by the rate of diffusion of Cr in the matrix alloy. In the other process, carbide precipitation of both Fe and Cr occurs. The decrease in Cr fraction in the carbide with the decrease in temperature indicates that the driving force for co-precipitation of Fe increases over that for Cr diffusion as temperature is lowered. Below a certain temperature (~450 °C), the rate of Cr diffusion is slow so that the carbide that precipitates has a composition that approaches that of the matrix. That is, the driving force for carbide precipitation is so great that it overrides Cr diffusion processes. Once Fe carbide forms, there is not a sufficient driving force for Cr to replace Fe in the carbide, so no Cr enrichment of Fe carbide occurs over time.

The observation that the chromium fraction in the precipitate is the same as the matrix alloy for low temperature aging has an important implication for LTS of weld HAZ. That is, no chromium depletion occurs as a result of LTS below the break temperature (~450 °C). Consequently, LTS by chromium depletion might not occur for aging below about 450 °C. The existence of a critical LTS temperature is confirmed by the stress corrosion cracking tests we performed on welded specimens that were aged at low temperatures. That is, no cracking was observed in the CERT's or CT tests on weld HAZ with LTS heat treatments at 360 °C or below in water environments at 288 °C with 0.2 ppm O_2 or at 180 °C with 1.0 ppm O_2. The difference in the critical LTS temperature for sensitization (450 °C) and IGSCC (360 °C) indicates that chromium depletion is not the sole consideration in modeling the effect of LTS heat treatment on IGSCC susceptibility. Other factors, such as grain boundary impurity segregation, may be of first-order importance in characterizing the detrimental effects of LTS. Further investigation is needed to identify fully these factors.

V. SUMMARY AND CONCLUSIONS

1. The chromium content of $M_{23}C_6$ carbides decreases with decreasing sensitization temperature. The low chromium content of carbides from LTS heat treatments at very low temperatures (<450 °C) suggests that the chromium depleted zones that result from LTS heat treatments have little or no width. The practical significance of this result is the indication that no significant chromium depletion will occur at grain boundaries as a result of long term (~40 year) exposures to BWR operating temperatures (288 °C).
2. For the 180 °C/1.0 ppm O_2 and 288 °C/0.2 ppm O_2 environments (simulated BWR start-up and steady-state environments), the highest crack growth rates were obtained from weld HAZ's with LTS heat treatments at 500° and 400 °C. The 385 °C LTS heat treatments produced significantly lower IGSCC rates. No IGSCC was observed from LTS heat treatments at 360 °C and below in the simulated BWR water environments. The 288 °C/8 ppm O_2 environment produced IGSCC in all metallurgical conditions examined, including the as-welded condition.
3. The degree of sensitization of Type 304 stainless steel weld HAZ, as measured by the EPR test, increased with increasing LTS heat treatment temperature. Generally, the degree of sensitization increased with increasing heat-treatment time; however, this trend was punctuated by one or two maxima and minima. The temperature dependence of sensitization suggests that chromium matrix or grain boundary diffusion is not the rate controlling process.

ACKNOWLEDGMENTS

This research was performed for the BWR Owner's Group under EPRI Contract T110-1. Technical advice from M. J. Fox, R. L. Jones, and B. C. Syrett and J. C. Danko of EPRI is appreciated. The microscopy performed at Stanford University by J. Rayment and R. Sinclair and at the University of Cincinnati by J. Moteff and R. Nekkanti is also appreciated.

REFERENCES

1. General Electric Company, Palo Alto, CA, Electric Power Research Institute, Final Report for Project 449-2, A J Giannuzzi, principal investigator, Dec 1978, NP-944.
2. General Electric Company, Palo Alto, CA, Electric Power Research Institute, Final Report for Project 1332-1, F P. Ford, principal investigator, Sept. 1982, NP-2589.
3. J. C. Danko: from *Proceedings. Second Seminar on Countermeasures for Pipe Cracking in BWRs*, Volume 3, *Remedy Application*, organized by J. C. Danko, Palo Alto, CA, Nov. 15–18, EPRI NP-3684-SR, p. 1-1.
4. C. Stawström and M. Hillert: *Journal of the Iron and Steel Institute*, 1969, vol 207, pp. 77-85
5. E C Bain, R H Aborn, and J B. Rutherford. *Trans Am. Soc. Steel Treatment*, 1933, vol. 21, pp. 481-509.
6. C S. Tedmon, D A Vermilyea, and J. H Rosolowski: *Journal of the Electrochemical Society*, 1971, vol. 118, pp 192-202
7. J S. Armijo *Corrosion*, 1968, vol. 24, pp. 24-30.
8. K. T Aust: *Trans AIME*, 1969, vol. 245, pp. 2117-26.
9. A. Joshi and D. F. Stein. *Corrosion*, 1972, vol 28, pp. 321-30.
10. M J. Povich: *Corrosion*, 1978, vol. 34, pp. 60-65

11. M. J. Povich and R. Rao: *Corrosion*, 1978, vol. 34, pp. 269-75.
12. W. L. Clarke, R. L. Cowan, and W. L. Walker: in *Intergranular Corrosion of Stainless Alloys*, ASTM STP 656, R. F. Steigerwald, ed., American Society for Testing and Materials, 1978, pp. 99-132.
13. ASTM Specifications E647-83, paragraph 9, *Annual Book of ASTM Standards*, Philadelphia, PA, 1983.
14. A. Saxena and S. J. Hudak, Jr.: *Int. J. Fracture*, 1978, vol. 14, pp. 453-68.
15. P. L. Andresen: Palo Alto, CA, Electric Power Research Institute, Seminannual Report 2 for EPRI Project T-115-3, Dec. 1980.
16. General Electric Company, Palo Alto, CA, Electric Power Research Institute, GE Final Report on EPRI Project 1972-1, May 1981, NP-1823.
17. General Electric Company, Palo Alto, CA, Electric Power Research Institute, GE Final Report for EPRI Project T118-1, July 1982, vols. 1 and 2, NP-2472-SY.
18. C. Da Casa, V. B. Nileshwar, and D. A. Melford: *Journal of the Iron and Steel Institute of London*, 1969, vol. 207, pp. 1325-32.
19. J. Philibert, G. Henry, M. Robert, and J. Pineau: *Mem. Sci. Rev. Met.*, 1961, vol. 58, p. 557.